DOA ESTIMATION WITH HEXAGONAL ARRAYS

Zhi Tian, Harry L. Van Trees

C3I Center
George Mason University
Fairfax, VA 22030

ABSTRACT

Hexagonal arrays are widely used in practice but have received less attention in the optimum array processing literature. In this paper, we show how unitary ESPRIT can be applied to hexagonal arrays for direction-of-arrival (DOA) estimation. The resulting estimates exhibit good threshold behavior, and are close to the Cramer-Rao bound above threshold. We also show how to use spatial smoothing in hexagonal arrays for DOA estimation in the presence of coherent signals.

1. INTRODUCTION

Hexagonal Arrays are widely implemented in practice. The elements in hexagonal arrays are arranged in concentric circles. This configuration is desirable whenever the desired beampattern is circularly symmetric. From another viewpoint, hexagonal sampling is proved to be the optimal sampling strategy for signals that are bandlimited over a circular region of the Fourier plane. For such signals hexagonal sampling requires 13.4 percent fewer samples than rectangular sampling [1]. These favorable characteristics of hexagonal arrays lead to their wide applications in practice. On the other hand, there is relatively little research work on hexagonal arrays in the array processing literature.

This paper studies the direction-of-arrival (DOA) estimation problems with hexagonal arrays. For 2-D planar arrays, not all the DOA estimation algorithms developed for linear arrays can be applied easily, for either mathematical or computational reasons. Algorithms such as maximum likelihood estimation are computationally too complex to be implemented in two-dimensional estimation problems. Simpler algorithms, such as spectral MUSIC, exhibit poor threshold behavior. Algorithms with direct solutions, on the other hand, are computationally much easier, and generally offer better performance in linear cases. Existing direct-solution algorithms for DOA estimation with uniform linear arrays include Root-MUSIC [2] and ESPRIT [3][4][5]. Ottersten et al [6] analyzed the performance of TLS ESPRIT and introduced a weighted version which results in performance very close to the Cramer-Rao bound when the algorithm is above threshold. However, due to the fact that the fundamental theorem of algebra does not hold in two dimensions, it is typically hard to find a direction-solution formulation for 2-D problems. There has been some work on 2-D polynomials (e.g. Hatkel et al) but they are not used in practice.

ESPRIT is a high-resolution signal parameter estimation technique based on the translational invariance structure of a sensor array. The parameter estimates are obtained by exploiting the rotational invariance structure of the signal subspace. Among the ESPRIT-like estimation schemes, Unitary ESPRIT [7] provides increased estimation accuracy with a reduced computational burden. By exploiting the conjugate symmetric property of the array manifold, Unitary ESPRIT utilizes a unitary transformation to map Centro-Hermitian matrices into real matrices. This transformation not only reduces computations by using real-valued computation throughout, but also implicitly embeds the forward-backward averaging, which uses the data samples more efficiently and gives improvement for correlated sources. The advantage of forward-backward averaging has been previously discussed by Linebarger et al [9].

The unitary ESPRIT algorithm can also be extended to two-dimensional DOA estimation with uniform rectangular arrays [8]. However, since the 2-D unitary ESPRIT was basically derived as a mathematical extension of linear results, its original formulation only applies to the cases of two orthogonal ULA's having a common phase center, namely, rectangular arrays.

This paper extends the unitary ESPRIT technique to hexagonal array geometry. In section 2, we introduce a hexagonal-rectangular transformation, which enables the possible extension of rectangular-grid results to hexagonal-grid arrays. A Unitary ESPRIT formulation for hexagonal arrays is developed in section 3. Section 4 discusses the application of spatial smoothing technique to hexagonal arrays. Simulation results are presented in section 5 to verify the efficiency of the 2-D unitary ESPRIT and spatially smoothed Unitary ESPRIT for hexagonal arrays. Section 6 summarizes our results.

2. HEXAGONAL-RECTANGULAR TRANSFORMATION

Consider a standard hexagonal array. We can define the array manifold vector by stacking the transposes of the row vectors of array into a column. The directions of signal arrivals can be expressed by the directional cosines with respect to each axis in **v** space as $v_x = \sin\theta\cos\phi$ and $v_y = \sin\theta\sin\phi$. In order to apply the rectangular results, we transform the hexagonal array into an equivalent rectangular-grid array using a transformation due to Lo and Lee [10]. We use the estimation algorithms on the rectangular grid array in (u_x, u_y) space and then find the corresponding estimates in (v_x, v_y) space.

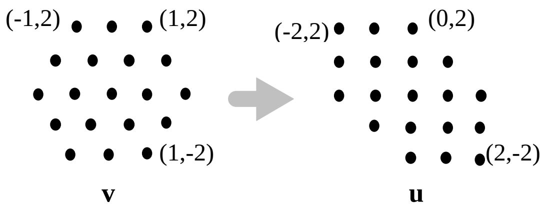

Figure 1. Hexagonal-rectangular transformation

The hexagonal-rectangular grid transformation depicted in Figure 1 can be expressed by

$$\mathbf{u} = \begin{bmatrix} 1 & 0 \\ -\frac{1}{\sqrt{3}} & \frac{2}{\sqrt{3}} \end{bmatrix} \mathbf{v}. \tag{1}$$

3. UNITARY ESPRIT[1]

3.1 Invariance Relationship

The basic idea of the ESPRIT technique is to exploit the shift invariance property of the associated array. For unitary ESPRIT, the array manifold is further required to be Centro-symmetric, which dictates the phase center to be chosen at the array center. The indexing in (u_x, u_y) space in the above section satisfies this condition. For a 19-element hexagonal array, the corresponding array manifold vector in rectangular grid is given by the 19×1 vector

$$\mathbf{v}_H(u_x, u_y) = e^{j\pi(\mathbf{n}_x u_x + \mathbf{n}_y u_y)} \tag{2}$$

with

$\mathbf{n}_x = [-2\ -1\ 0\ -2\ -1\ 0\ 1\ -2\ -1\ 0\ 1\ 2\ -1\ 0\ 1\ 2\ 0\ 1\ 2]^T$,

$\mathbf{n}_y = [2\ 2\ 2\ 1\ 1\ 1\ 1\ 0\ 0\ 0\ 0\ 0\ -1\ -1\ -1\ -1\ -2\ -2\ -2\ ]^T$.

$\mathbf{v}_H(u_x, u_y)$ can be transformed into a real-valued array manifold by using a unitary matrix $\mathbf{Q}_N$, that is,

$$\mathbf{v}_R(u_x, u_y) = \mathbf{Q}_N^H \mathbf{v}_H(u_x, u_y) \tag{3}$$

where $\mathbf{Q}_N$ is defined as

$$\mathbf{Q}_{2K} = \begin{bmatrix} \mathbf{I}_K & j\mathbf{I}_K \\ \mathbf{II}_K & -j\mathbf{II}_K \end{bmatrix} \tag{4}$$

for N even, and

$$\mathbf{Q}_{2K+1} = \begin{bmatrix} \mathbf{I}_K & \mathbf{0} & j\mathbf{I}_K \\ \mathbf{0}^T & \sqrt{2} & \mathbf{0}^T \\ \mathbf{II}_K & \mathbf{0} & -j\mathbf{II}_K \end{bmatrix} \tag{5}$$

for N odd. $\mathbf{II}_K$ is the K×K exchange matrix.

Similar to unitary ESPRIT for uniform linear arrays, we need to construct two identical subarrays that reveal the translational invariance relationship. Instead of constructing just one pair of subarrays, as in linear case, we need two pairs of subarray selection matrices to present the shift invariances for signal directions in both x-axis and y-axis, respectively. Moreover, in order to have real-valued computation from start to finish, subarrays shall be symmetrically selected to each other with respect to the array center. For u_x, these two requirements for unitary ESPRIT formulation can be expressed as follows:

$$e^{j\pi u_x} \mathbf{J}_{x1} \mathbf{v}_H(u_x, u_y) = \mathbf{J}_{x2} \mathbf{v}_H(u_x, u_y) \tag{6}$$

$$\mathbf{II}_M \mathbf{J}_{x2} \mathbf{II}_N = \mathbf{J}_{x1} \tag{7}$$

Subarray selection matrices $\mathbf{J}_{x1}$, $\mathbf{J}_{x2}$ as in (6) pick out M rows of array manifold $\mathbf{v}_H(u_x, u_y)$ where M is the number of elements in each subarray. Graphically, the subarray selection matrix can be denoted by Figure 2. For example, $\mathbf{J}_{x2}$ selects the following 14 elements:

2 3
5 6 7
9 10 11 12
14 15 16
18 19

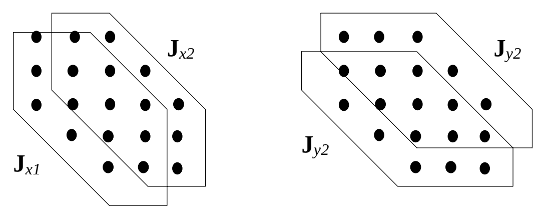

Figure 2. Subarrays for unitary ESPRIT

It is easy to verify that the above two pairs of subarray selection structures contain the information about the shift invariances of u_x and u_y, respectively, and that they all have the symmetry property required by unitary transformation. Therefore, unitary ESPRIT algorithm can be implemented using these two structures.

3.2 Development of Unitary ESPRIT

We start with the shift invariance relationship for u_x. When relationships in (6), (7) hold, it follows that the real-valued array manifold $\mathbf{v}_R(u_x, u_y)$ satisfies the following relation:

$$\tan(\frac{u_x}{2}) \mathbf{K}_{x1} \mathbf{v}_R(u_x, u_y) = \mathbf{K}_{x2} \mathbf{v}_R(u_x, u_y) \tag{8}$$

where $$\mathbf{K}_{x1} = \mathrm{Re}\{\mathbf{Q}_M^H \mathbf{J}_{x2} \mathbf{Q}_N\} \tag{9}$$

$$\mathbf{K}_{x2} = \mathrm{Im}\{\mathbf{Q}_M^H \mathbf{J}_{x2} \mathbf{Q}_N\} \tag{10}$$

Similarly, for u_y, we have

$$\tan(\frac{u_y}{2}) \mathbf{K}_{y1} \mathbf{v}_R(u_x, u_y) = \mathbf{K}_{y2} \mathbf{v}_R(u_x, u_y) \tag{11}$$

$$\mathbf{K}_{y1} = \mathrm{Re}\{\mathbf{Q}_M^H \mathbf{J}_{y2} \mathbf{Q}_N\} \tag{12}$$

$$\mathbf{K}_{y1} = \mathrm{Im}\{\mathbf{Q}_M^H \mathbf{J}_{y2} \mathbf{Q}_N\} \tag{13}$$

[1] To compress our development, we assume the reader is familiar with [8].

Consider the N×D real-valued array manifold matrix $\mathbf{V}_R(\mathbf{u}_x,\mathbf{u}_y)=[\mathbf{v}_R(u_{x1},u_{y1}),\cdots,\mathbf{v}_R(u_{xD},u_{yD})]$, it can be easily shown that $\mathbf{V}_R(\mathbf{u}_x,\mathbf{u}_y)$ satisfies

$$\mathbf{K}_{x1}\mathbf{V}_R(\mathbf{u}_x,\mathbf{u}_y)\Omega_x=\mathbf{K}_{x2}\mathbf{V}_R(\mathbf{u}_x,\mathbf{u}_y) \quad (14)$$

$$\mathbf{K}_{y1}\mathbf{V}_R(\mathbf{u}_x,\mathbf{u}_y)\Omega_y=\mathbf{K}_{y2}\mathbf{V}_R(\mathbf{u}_x,\mathbf{u}_y) \quad (15)$$

where $$\Omega_x=diag\{\frac{u_{x1}}{2},\cdots,\frac{u_{xD}}{2}\} \quad (16)$$

$$\Omega_y=diag\{\frac{u_{y1}}{2},\cdots,\frac{u_{yD}}{2}\} \quad (17)$$

We utilize the signal subspace that spans the same column space as array manifold $\mathbf{V}_R(\mathbf{u}_x,\mathbf{u}_y)$. If we define

$$\mathbf{R}_q\triangleq\mathrm{Re}\{\mathbf{Q}_N^H\mathbf{R}_x\mathbf{Q}_N\}=\mathbf{Q}_N^H\mathbf{R}_{x,FB}\mathbf{Q}_N \quad (18)$$

and denote the largest D eigenvectors of $\mathbf{R}_q$ as $\mathbf{E}_s$, it follows that $\mathbf{E}_s=\mathbf{V}_R\cdot\mathbf{T}$ where $\mathbf{T}$ is a non-singular matrix. Therefore, Equations (14), (15) can be rewritten in terms of the signal subspace matrix $\mathbf{E}_s$ as follows:

$$\mathbf{K}_{x1}\mathbf{E}_s\Psi_x=\mathbf{K}_{x2}\mathbf{E}_s \quad (19)$$

$$\mathbf{K}_{y1}\mathbf{E}_s\Psi_y=\mathbf{K}_{y2}\mathbf{E}_s \quad (20)$$

where $\Psi_x=\mathbf{T}^{-1}\Omega_x\mathbf{T}$, $\Psi_y=\mathbf{T}^{-1}\Omega_y\mathbf{T}$.

Automatic pairing of $\mathbf{u}_x$ and $\mathbf{u}_y$ can be achieved by observing that the spatial frequency estimates of $\mathbf{u}_x$ and $\mathbf{u}_y$ can be obtained from the eigenvalues of the real and imaginary part of $\Psi_x+j\Psi_y$, respectively.

To summarize, unitary ESPRIT algorithm works for hexagonal arrays as follows:

1) Compute signal subspace $\mathbf{E}_s$ via a real-valued eigen-decomposition of the matrix $\mathbf{R}_q=\mathrm{Re}\{\mathbf{Q}_N^H\mathbf{R}_x\mathbf{Q}_N\}$,
2) Compute Ψ_x,Ψ_y as the solutions to the matrix equations in (19), (20),
3) Compute λ_i , i = 1,…,D as the eigenvalues of the D ×D matrix $\Psi_x+j\Psi_y$,
4) For i = 1,...,D, compute estimates $u_{xi}=2\tan^{-1}(\mathrm{Re}\{\lambda_i\})$, $u_{yi}=2\tan^{-1}(\mathrm{Im}\{\lambda_i\})$.

4. SPATIAL SMOOTHING FOR HEXAGONAL ARRAYS

Spatial smoothing is a technique of removing signal coherency and reducing signal correlation by preprocessing the data set.

For a 19-element hexagonal array, we construct a set of L subarrays of M elements, as shown in Figure 3. Each subarray is shifted by one in both x and y direction from the preceding subarray.

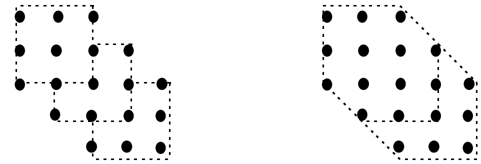

(a) L=3, M=9 (b) L=2, M=14

Figure 3. Subarrays for spatially smoothed Unitary ESPRIT

Since each subarray structure is symmetric with respect to its center, we can implement unitary ESPRIT algorithm on the subarray after spatial smoothing. Notice that the first subarray structure has unitary ESPRIT working on a rectangular array manifold, while the second on a 14-element hexagonal-like subarray. Following the idea of constructing subarray selection matrix for hexagonal arrays, 2-D unitary ESPRIT algorithm can be easily adapted for any symmetric arrays in parallelogram-like grid.

5. SIMULATIONS

Computer simulations were performed using a 19-element standard hexagonal array with elements spaced half a wavelength apart. The impinging signals consist of two equi-powered, uncorrelated sources located at (0,0) and (0,0.0866) in (v_x,v_y) space, respectively. The effect of unitary ESPRIT on the resulting signal estimates was examined using 100 snapshots and 500 trials. Figure 4 depicts the resulting root mean square error (RMSE) versus the signal-to-noise ratio (SNR), as compared to the Cramer-Rao bound for the hexagonal array. Unitary ESPRIT approaches the Cramer-Rao bound rapidly above 0 dB SNR. Just as in the linear case, the asymptotic estimation error of ESPRIT is parallel to the Cramer-Rao bound with a small offset.

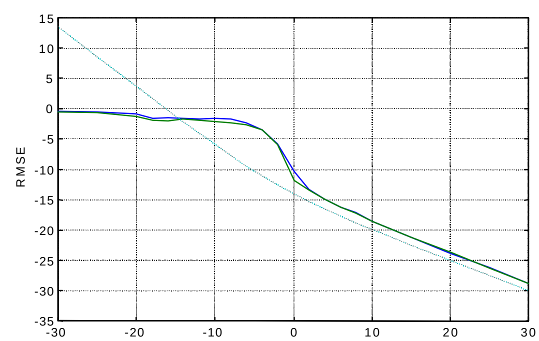

Figure 4. Performance of unitary ESPRIT vs. SNR: Root MSE (19-element hexagonal array)

To investigate the effect of spatial smoothing technique on hexagonal arrays, we use two coherent signals from the same sources as above. It can be seen from Figure 5 that, without spatial smoothing, unitary ESPRIT technique cannot handle the coherency. Simulation shows that the subarray structure in Figure 3 (a) outperforms that in Figure 3 (b) by about 0.5 dB.

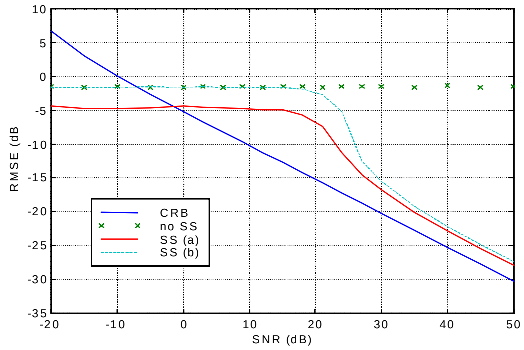

Figure 5. Performance of spatial smoothing technique versus SNR: signal separation = 0.0866, $\rho = 1$, $\phi_\rho = 0^o$.

Tests were also conducted on the performance of spatial smoothing for correlated signals by evaluating the root mean square error versus the magnitude of signal correlation, as shown in Figure 6. When the correlation phase equals 0 and $|\rho|$ is greater than 0.99, the estimation error of unitary ESPRIT increases dramatically, while spatial smoothing can still handle the highly correlated situation. When the correlation phase is 90^o, unitary ESPRIT resolves the signals for any correlation magnitude as shown in Figure 6(b). The forward-backward averaging scheme embedded in unitary ESPRIT decorrelates the two signals without spatial smoothing. While the spatial smoothing technique reduces signal correlation, it sacrifices resolution by working on a reduced-dimension subarray.

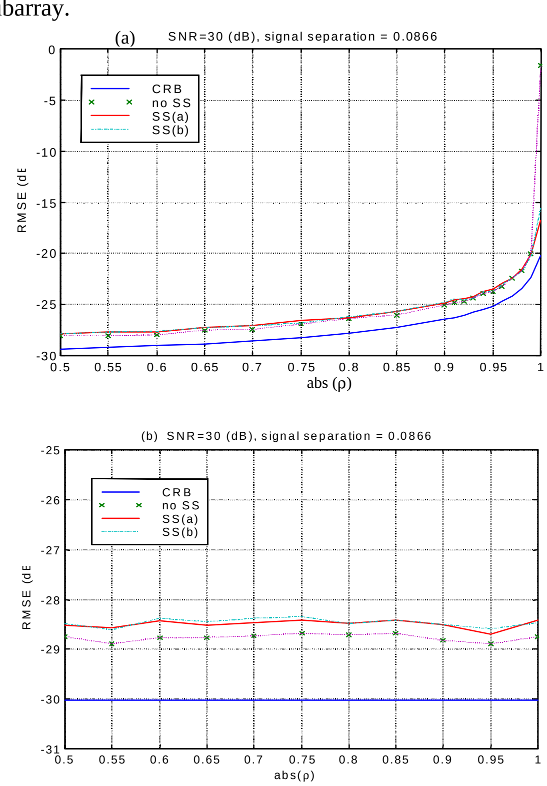

Figure 6. Performance of spatial smoothing versus signal correlation: (a) $\phi_\rho = 0^o$, (b) $\phi_\rho = 90^o$

6. CONCLUSIONS

Unitary ESPRIT provides a computationally efficient DOA estimation algorithm for hexagonal arrays. The threshold behavior is good and the mean-square error is close to the Cramer-Rao bound above threshold. Spatial smoothing coupled with unitary ESPRIT provides an effective solution for coherent signals.

By using techniques similar to those in [8] and the transformation in section 2, a beamspace version of unitary ESPRIT for hexagonal arrays can be derived.

REFERENCES

[1] Petersen, D. P., and Middleton, D., "Sampling and reconstruction of wave-number-limited functions in N-dimensional Eulidean spaces," Inform. Contr., vol.5, pp. 279-323, 1962.

[2] Barabell, A. J., "Improving the resolution performance of eigenstructure-based direction-finding algorithms," Proc. IEEE Int. Conf. Acoust., Speech, Signal Processing, pp. 336-339, 1983.

[3] Roy, R., "ESPRIT-estimation of signal parameters via rotational invariance techniques," Ph.D. thesis, Stanford University, August 1987.

[4] Roy, R., and Kailath, T., "ESPRIT-estimation of signal parameters via rotational invariance techniques," IEEE Trans. Acoust., Speech, and Sig. Proc., vol. 37, pp. 984-995, July 1989.

[5] Roy, R., "Esprit-Estimation of signal parameters via rotational invariance techniques," IEEE Trans. on Signal Processing, vol. 40, pp. 867-881, April 1992.

[6] Ottersten, B., Viberg, M., and Kailath, T., "Performance analysis of the total least squares ESPRIT algorithm," IEEE Trans. Signal Processing, vol. 39, pp. 1122-1135, May 1991.

[7] Haardt, M., and Nossek, J. A., "Unitary ESPRIT: How to obtain increased estimation accuracy with a reduced computational burden," IEEE Trans. on Signal Processing, vol. 43, pp.1232-1242, May 1995.

[8] Zoltowski, M. D., Haardt, M., and Mathews, C. P., "Closed-form 2-D angle estimation with rectangular arrays in element space or beamspace via unitary ESPRIT," IEEE Trans. on Signal Processing, vol. 44, pp. 316-328, February 1996.

[9] Linebarger, D. A., DeGroat, R. D., and Dowling, E. M., "Efficient direction-finding methods employing forward/backward averaging," IEEE Trans. Signal Processing, vol. 42, pp. 2136-2145, August 1994.

[10] Lo, V. T., and Lee, S. W., "Affine transformation and its application to antenna arrays," IEEE Trans. Antennas Propag., vol. AP-13, pp. 890-896, 1965.